Inorganic Chemistry
Article

*Inorg. Chem.* **2010**, *49*, 8769–8778 **8769**
DOI: 10.1021/ic1009797

# Electron Paramagnetic Resonance Studies of Nitrosyl and Thionitrosyl and Density Functional Theory Studies of Nitrido, Nitrosyl, Thionitrosyl, and Selenonitrosyl Complexes of Chromium

**Johannes R. Dethlefsen, Anders Døssing,* and Erik D. Hedegård**

*Department of Chemistry, University of Copenhagen, Universitetsparken 5, DK-2100 Copenhagen Ø, Denmark*

Received May 17, 2010

The novel $S = 1/2$ thionitrosyl complexes $Cr(NS)(CN)_5^{3-}$, $Cr(NS)(dmso)_5^{2+}$, and $Cr(NS)(nmf)_5^{2+}$ (dmso = dimethyl sulfoxide, nmf = *N*-methylformamide) have been prepared, and their optical and electron paramagnetic resonance (EPR) spectra were studied. The values of the isotropic and anisotropic hyperfine and superhyperfine coupling constants $A(^{53}Cr)$, $A(^{14}N)$, and $A(^{13}C)$ and of $g$ were determined from the EPR spectra at room temperature and at 66 K. The values of $A_\perp$ and $A_{iso}$ in the thionitrosyl complexes were slightly higher than in the analogous nitrosyl complexes. A common feature in the optical absorption spectra of the thionitrosyl complexes in solution at 298 K is an absorption band around 600 nm with a vibronic structure whereas such a band is located around 450 nm in the analogous nitrosyl complexes. Density functional theory (DFT) studies of the series of complexes $Cr(N)(H_2O)_5^{2+}$, $Cr(NO)(H_2O)_5^{2+}$, $Cr(NS)(H_2O)_5^{2+}$, and $Cr(NSe)(H_2O)_5^{2+}$ show that the unpaired electron resides in a metal-based $d_{xy}$ orbital and that the electronic structure in the equatorial plane is similar in all four complexes and similar to $Cr^{3+}$. The $\sigma$ donating ability was found in the order $N^{3-} \gg NO < NS \approx NSe$ and the $\pi$ accepting ability in the order $NO > NS \approx NSe$. Time dependent DFT calculations gave in all four complexes a $d_{x^2-y^2} \leftarrow d_{xy}$ transition energy around 17 500 $cm^{-1}$.

## Introduction

Nitrogen monosulfide (NS) is isovalent with nitric oxide (NO) with one unpaired electron. NO is a stable gas at room temperature whereas NS is a very reactive radical that readily polymerizes, and it can only be studied at very low pressure in the gas phase. One notable difference between the NS and the NO molecule is the much higher electric dipole moment for NS ($\mu = 1.83$ D)[1] with the negative charge residing on the nitrogen atom compared to NO with $\mu = 0.16$ D.[2] NS can be stabilized by coordination to a metal center by the formation of a thionitrosyl complex $M(NS)L_n^z$. The first thionitrosyl complex $Mo(NS)(S_2CNR_2)_3$ was isolated by Chatt in 1974,[3] and compared to the number of isolated nitrosyl complexes $M(NO)L_n^z$ the number of well-characterized thionitrosyl complexes is low with most of them being of the middle second and third row transition metals.[4] Among the few first row transition metal thionitrosyl complexes is the blue $S = 1/2$ complex $[Cr(NS)(CH_3CN)_5](PF_6)_2$ reported by Herberhold and Haumaier.[5] Recently, it was shown that photolysis of this complex in $CH_3CN$ solution results in a dissociation of NS,[6] a behavior similar to the nitrosyl complexes where a release of NO commonly is observed upon irradiation. Another study[7] showed that the $CH_3CN$ ligands easily can be substituted with $H_2O$ ligands with the formation of the green complex $Cr(NS)(H_2O)_5^{2+}$ as a result. By comparison with the optical spectra of the well-known complex $Cr(NO)(H_2O)_5^{2+}$,[8] it was concluded that the NO and NS ligands display very different spectrochemical properties. This is, however, not surprising given the much higher electron density on the nitrogen atom in NS than in NO.

It is well-known that the assignment of a formal oxidation state of the metal center in transition metal nitrosyl complexes $M(NO)L_n^z$ is ambiguous. In the Enemark-Feltham notation, an M(NO) core can be designated $\{M(NO)\}^n$ where $n$ is the total number of electrons in the metal d orbitals and $\pi^*$ orbitals of the NO ligand, and this notation has proved useful with regard to a rationalization of the coordination geometry of the M(NO) core (bent vs linear).[9] In this notation, the complex $Cr(NO)(H_2O)_5^{2+}$ should be designated $\{Cr(NO)\}$.[5] This oxidation state ambiguity has recently been addressed in two papers by Gray et al.[10,11] who employed

*To whom correspondence should be addressed. E-mail: dossing@kiku.dk.

(1) Byfleet, C. R.; Carrington, A.; Russel, D. K. *Mol. Phys.* **1971**, *20*, 271–277.
(2) Liu, Y.; Guo, Y.; Lin, J.; Huang, G.; Duan, C.; Li, F. *Mol. Phys.* **2001**, *99*, 1457–1461.
(3) Chatt, J.; Dilworth, J. R. *J. Chem. Soc., Chem. Commun.* **1974**, 508.
(4) Pandey, K. K. *Prog. Inorg. Chem.* **1992**, *40*, 445–503.
(5) Herberhold, M.; Haumaier, L. *Z. Naturforsch.* **1980**, *35B*, 1277–1280.
(6) Dethlefsen, J. W.; Hedegård, E. D.; Rimmer, R. D.; Ford, P. C.; Døssing, A. *Inorg. Chem.* **2009**, *48*, 231–238.
(7) Dethlefsen, J. W.; Døssing, A. *Inorg. Chim. Acta* **2009**, *362*, 259–262.
(8) Døssing, A.; Frey, A. M. *Inorg. Chim. Acta* **2006**, *359*, 1681–1684.
(9) Enemark, J. H.; Feltham, R. D. *Coord. Chem. Rev.* **1974**, *13*, 339–406.
(10) Hummel, P.; Gray, H. B. *Coord. Chem. Rev.* **2007**, *251*, 554–556.
(11) Hummel, P.; Winkler, J. R.; Gray, H. B. *Theor. Chem. Acc.* **2008**, *119*, 35–38.


Published on Web 08/30/2010

density functional theory (DFT) to study the electronic structures of the tetragonal $n = 6$ nitrosyl $M(NO)L_5^z$ and $d^2$ nitrido $M(N)L_5^z$ complexes of the group 7 and 8 metals with L = $NH_3$ and $CN^-$. These studies revealed that the electronic structures of the $M(NO)L_5^z$ and $M(N)L_5^z$ complexes are very similar, and that the low-oxidation-state-metal/$NO^+$ formulation of transition metal nitrosyl complexes is incorrect.

On this background we report here the preparation of the novel thionitrosyl complexes $Cr(NS)(dmso)_5^{2+}$ (dmso = dimethyl sulfoxide), $Cr(NS)(nmf)_5^{2+}$ (nmf = *N*-methylformamide), and $Cr(NS)(CN)_5^{3-}$ (all $\{Cr(NS)\}^5$ complexes) along with their optical and electron paramagnetic resonance (EPR) spectra. To obtain more information about the electronic structures of the thionitrosyl chromium complexes we have also carried out DFT calculations on the complex $Cr(NS)(H_2O)_5^{2+}$, and have for comparison included the complexes $Cr(N)(H_2O)_5^{2+}$, $Cr(NO)(H_2O)_5^{2+}$, and $Cr(NSe)(H_2O)_5^{2+}$ in the calculations.

## Experimental Section

**Materials.** The compounds $[Cr(NS)(CH_3CN)_5](PF_6)_2$ and $[Cr(NO)(CH_3CN)_5](PF_6)_2$ were prepared by literature methods.[5,12] Dimethyl sulfoxide (ACS spectrophotometric grade) and *N*-methylformamide (nmf) were purchased from Sigma-Aldrich and used as received. Sodium cyanide ($^{13}C$, 99%) was purchased from Cambridge Isotope Laboratories.

**Preparation of $[Cr(NS)(dmso)_5](PF_6)_2$.** To a solution of $[Cr(NS)(CH_3CN)_5](PF_6)_2$ (0.60 g, 1.0 mmol) in deoxygenated dmso (5 mL) that had equilibrated for 35 min, ethyl acetate (60 mL) was added over 15 min. The resulting green precipitate was filtered off, washed with ethyl acetate (2 × 40 mL) and diethyl ether (2 × 40 mL), and dried in vacuo. Yield: 0.59 g of $[Cr(NS)(dmso)_5](PF_6)_2$ (0.76 mmol, 76%). Anal. Calc. (%) for $C_{10}H_{30}NCrF_{12}O_5P_2S_6$: C, 15.43; H, 3.84; N, 1.80; Cr. 6.68; S, 24.71. Found: C, 15.29; H, 3.84; N, 1.74; Cr. 6.59; S, 24.7. IR (KBr pellet) 1265 $cm^{-1}$, (dmso) 1261 $cm^{-1}$ ($\nu_{NS}$). UV−vis in dmso ($\lambda_{max}$/nm, $\varepsilon/M^{-1}$ $cm^{-1}$): (621, 62), (447, 132).

**Solution Preparation.** All solutions for EPR spectroscopy had a chromium concentration in the range 0.02−0.03 M. The EPR spectrum of $[Cr(NS)(dmso)_5](PF_6)_2$ at room temperature was recorded in neat dmso. For the frozen glass spectrum, the same volume of butane-2,3-diole was added to the solution, and the mixture was immediately cooled to 66 K. Solutions for room temperature EPR spectra of $Cr(NE)(nmf)_5^{2+}$ (E = O, S) were prepared by dissolving $[Cr(NE)(CH_3CN)_5](PF_6)_2$ in nmf, and the mixture was equilibrated at room temperature for 4 h prior to the measurements. For the frozen glass spectra, toluene was added to the equilibrated solution ($V_{nmf}:V_{toluene}$ = 3:1) and the mixture was immediately cooled to 66 K. Solutions for room temperature EPR spectra of $Cr(NE)(CN)_5^{3-}$ (E = O, S) were prepared by dissolving $[Cr(NE)(CH_3CN)_5](PF_6)_2$ in dmso saturated with NaCN (or $Na^{13}CN$), and the mixture was equilibrated at room temperature for 2 h prior to the measurements. For the frozen glass spectra, methanol was added to the equilibrated solution ($V_{dmso}:V_{methanol}$ = 1:2) and the mixture was immediately cooled to 66 K. Deoxygenated solutions for the optical absorption spectra were prepared by applying standard cannula techniques. Solutions for the absorption spectra of $Cr(NE)(CN)_5^{3-}$ were prepared by dissolving $[Cr(NE)(CH_3CN)_5](PF_6)_2$ in dmso saturated with NaCN. The solutions were equilibrated for 2 h. Solutions for the absorption spectra of $Cr(NE)(nmf)_5^{2+}$ were prepared by dissolving $[Cr(NE)(CH_3CN)_5](PF_6)_2$ in nmf. The solutions were equilibrated for 4 h. The solutions contained after equilibration only the fully substituted species $Cr(NE)L_5^z$ as judged from the EPR spectra of the solutions. The presence of partially substituted species $Cr(NE)(CH_3CN)_nL_{5-n}^z$ in the solutions would result in broad bands in the EPR spectra. Such EPR spectra were indeed observed during the equilibration.

**Instrumentation.** Optical absorption spectra were recorded on a Cary 5E UV−vis−NIR spectrophotometer. EPR spectra were recorded on a Bruker Elexsys E 500 instrument, operated at the X-band, equipped with a frequency counter and a Gauss-meter. The EPR spectra were fitted and simulated by use of a program written by Dr. H. Weihe (University of Copenhagen, 2007).[13]

**DFT Calculations.** All geometries in the series $Cr(X)(H_2O)_5^{2+}$ (X = N, NO, NS, NSe) were initially optimized. Geometry optimizations were performed with a TZV basis of Ahlrichs[14,15] and the BP86 functional,[16,17] within the Gaussian03 program package.[18] In all cases, tight SCF convergence criteria and an ultrafine grid were employed. A frequency analysis was carried out on all optimized geometries, and the absence of imaginary frequencies was used to confirm the minimum character of the optimized structures. We tried to extend the applied triple-ζ basis with polarization functions, but this was not tractable for the entire series and led in some cases to severe convergence difficulties. Different functionals were not invoked in geometry optimizations because of reports on related compounds,[11] which concluded that the effects on geometrical parameters from change of functional were small. From the optimized geometries, EPR hyperfine coupling constants (HFCCs) and transition energies (from time dependent DFT (TDDFT)) were calculated in the ADF[19] (ESR module) and ORCA[20] (CIS module) program packages, respectively. For the EPR parameters, we only report the results of one combination of basis set and functional (STO ccpVQZ and BP86). Many other variants were applied, but this will be the matter of a forthcoming publication. The TDDFT calculations were performed with three combinations of exchange and correlation functionals, namely, BP86, BLYP, and B3LYP.[17,21,22] The number of excited states was set to 25 with a Davidson dimension of 625. All orbitals were

(12) Clamp, S.; Connelly, N. G.; Taylor, G. E.; Louttit, T. S. *J. Chem. Soc., Dalton Trans.* **1980**, 2162–2169.

(13) (a) Bang, E.; Eriksen, J.; Glerup, J.; Mønsted, L.; Mønsted, O.; Weihe, H. *Acta Chem. Scand.* **1991**, *45*, 367–372. (b) Glerup, J.; Weihe, H. *Acta Chem. Scand.* **1991**, *45*, 444–448.

(14) Schäfer, A.; Horn, H.; Ahlrichs, R. *J. Chem. Phys.* **1992**, *97*, 2571–2577.

(15) Schäfer, A.; Huber, C.; Ahlrichs, R. *J. Chem. Phys.* **1994**, *100*, 5829–5835.

(16) Perdew, J. P. *Phys. Rev. B* **1986**, *33*, 8822–8824.

(17) Becke, A. D. *Phys. Rev. A* **1988**, *38*, 3098–3100.

(18) Frisch, M. J.; Trucks, G. W.; Schlegel, H. B.; Scuseria, G. E.; Robb, M. A.; Cheeseman, J. R.; Montgomery, J. A., Jr.; Vreven, T.; Kudin, K. N.;Burant, J. C.; Millam, J. M.; Iyengar, S. S.; Tomasi, J.; Barone, V.; Mennucci, B.; Cossi, M.; Scalmani, G.; Rega, N.; Petersson, G. A.; Nakatsuji, H.; Hada, M.; Ehara, M.; Toyota, K.; Fukuda, R.; Hasegawa,J.; Ishida, M.; Nakajima, T.; honda, Y.; Kitao, O.; Nakai, H.; Klene, M.; Li,X.; Knox, J. E.; Hratchian, H. P.; Cross, J. B.; Adamo, C.; Jaramillo, J.; Gomperts, R.; Stratmann, R. E.; Yazyev, O.; Austin, A. J.; Cammi, R.; Pomelli, C.; Ochterski, J. W.; Ayala, P. Y.; Morokuma, K.; Voth, G. A.; Salvador, P.; Dannenberg, J. J.; Zakrzewski, V. G.; Dapprich, S.; Daniels, A. D.; Strain, M. C.; Farkas, O.; Malick, D. K.; Rabuck, A. D.; Raghavachari,K.; Foresman, J. B.; Ortiz, J. V.; Cuiq, Q.; Baboul, A. G.; Clifford, S.;Cioslowski, J.; Stefanov, B. B.; Liu, G.; Liashenko, A.; Piskorz, P.; Komaromi, I.; Martin, R. L.; Fox, D. J.; Keith, T.; Al-Laham, M. A.; Peng,C. Y.; Nanayakkara, A.; Challacombe, M.; Pople, J. A. *Gaussian 03*, revisionC.02; Gaussian Inc.: Wallingford, CT, 2004.

(19) Velde, G. T.; Bickelhaupt, F. M.; Baerends, E. J.; Guerra, C. F.; van Gisbergen, S. J. A.; Snijders, J. G.; Ziegler, T. *J. Comput. Chem.* **2001**, *22*, 931–967.

(20) Neese, F. *ORCA-an ab initio, density functional and semiempirical program package*, version 2.6.71; University of Bonn: Bonn, Germany (http://www.thch.uni-bonn.de/tc/orca/).

(21) Lee, C.; Yang, W.; Parr, R. G. *Phys. Rev. B* **1988**, *37*, 785–788.

(22) Stephens, P. J.; Devlin, F. J.; Chabalowski, C. F.; Frisch, M. *J. Phys. Chem.* **1994**, *98*, 11623–11627.

included in the CIS procedure. Further, the RI and Tamm-Dancoff approximations were generally applied. As mainly transitions of profound d-d character are considered, the nature of these transitions was confirmed by the weight of the participating states and by plotting of the difference densities. Using only the BP86 functional on the compounds $Cr(N)(H_2O)_5^{2+}$ and $Cr(NO)(H_2O)_5^{2+}$, a series of calculations with TZV, TZVP, TZVPP, and QZVP basis sets were performed. This showed only small variations of the transition energies within the applied series of basis sets. To obtain consistency with preliminary calculations in the ADF program package (STO TZ2P basis and BP86 functional), results reported here are with TZVPP basis and BP86 functional. The BLYP and B3LYP results are compiled in Supporting Information (see Supporting Information Table S-6). Transition energies with BP86 and BLYP are in general found to be similar, but B3LYP leads for some transitions to significantly higher transition energies. Problems with spin contamination (see Supporting Information Table S-1), especially for the heavier chalcogens, were also observed with B3LYP. The effect of using Tamm-Dancoff and RI approximations had negligible impact on the obtained transition energies (see Supporting Information Tables S-2 and S-3). All molecular orbital (MO) diagrams in Figure 5 are constructed from the preliminary results with a triple-ζ STO basis (TZ2P) and the BP86 functional, calculated in ADF[23] (the used energies are shown in Supporting Information Table S-4). However, the orbital energy differences obtained in these calculations are almost identical with results obtained with the TZVPP basis. Of the reported population analyses, the Löwdin and Mulliken population analyses were calculated in ORCA, while the NBO program (version 3.1, implemented in Gaussian)[24−26] was used to obtain NPA charges. For consistency, all population analyses and corresponding charges are calculated with the BP86 functional and the TZVPP basis set. This basis set is not implemented as standard in the Guassian03 package, and has been imported manually from the Turbomole library.[27]

## Results and Discussion

**Syntheses and Optical and EPR Spectra.** The complexes $Cr(NS)(dmso)_5^{2+}$, $Cr(NS)(nmf)_5^{2+}$, and $Cr(NS)(CN)_5^{3-}$ were prepared by substitution of the labile acetonitrile ligands in the complex $Cr(NS)(CH_3CN)_5^{2+}$. Dissolution of $[Cr(NS)(CH_3CN)_5](PF_6)_2$ in neat dmso leads accordingly to a complete substitution after which the green complex $[Cr(NS)(dmso)_5](PF_6)_2$ can be precipitated. Large single-crystals of this complex could be grown but disorder prevented a satisfactory crystal structure determination. Dissolution of $[Cr(NS)(CH_3CN)_5](PF_6)_2$ in dmso saturated with NaCN leads to the formation of $Cr(NS)(CN)_5^{3-}$. This complex could not be isolated in the solid state. Analogously, dissolution of $[Cr(NS)(CH_3CN)_5](PF_6)_2$ in neat nmf gives the complex $Cr(NS)(nmf)_5^{2+}$ which was not isolated in the solid state. For comparison, solutions of the novel complex $Cr(NO)(nmf)_5^{2+}$ and of $Cr(NO)(CN)_5^{3-}$ were prepared in the same way from $[Cr(NO)(CH_3CN)_5](PF_6)_2$.

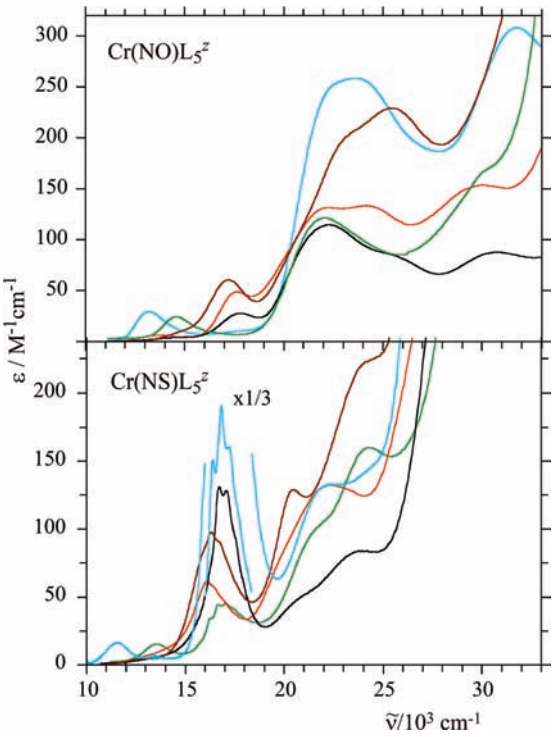


**Figure 1.** Optical absorption spectra at 298 K of the $Cr(NO)L_5^z$ (top) and $Cr(NS)L_5^z$ (bottom) complexes. L = $H_2O$ ($z$ = 2+, black), $CH_3CN$ ($z$ = 2+, blue), dmso ($z$ = 2+, red), nmf ($z$ = 2+, brown), $CN^-$ ($z$ = 3-, green). Absorption maxima ($\nu_{max}$/cm$^{-1}$, $\varepsilon$/M$^{-1}$ cm$^{-1}$): $Cr(NS)(CN)_5^{3-}$: (13 500, 15), (16 667, 44), (17 036, 45), (24 300, 132). $Cr(NO)(CN)_5^{3-}$: (14 600, 25), (22 000, 121). $Cr(NS)(nmf)_5^{2+}$: (16 300, 98), (20 500, 129). $Cr(NO)(nmf)_5^{2+}$: (17 200, 61), (25 300, 229). The absorption maxima for all the complexes are compiled in Table 1.

The optical absorption spectra of the complexes $Cr(NS)(dmso)_5^{2+}$, $Cr(NS)(nmf)_5^{2+}$, and $Cr(NS)(CN)_5^{3-}$ are shown in Figure 1, and transition energies are listed in Table 1. For comparison, the previously reported[7] spectra of the complexes $Cr(NS)(CH_3CN)_5^{2+}$ and $Cr(NS)(H_2O)_5^{2+}$ and of the analogous nitrosyl complexes[8,28] have been included. As seen in Figure 1, a common feature in the spectra of the $Cr(NO)L_5^z$ complexes is an absorption band located around 22 000 cm$^{-1}$ independent of the position of L in the spectrochemical series. At low temperature this band displays in some cases a vibrational progression. This band has been assigned as a $2e(d_{yz,zx},\pi^*_{NO})^* \leftarrow 1e(d_{yz,zx},\pi^*_{NO})$ transition located in the Cr(NO) core with the vibronic structure due to the Cr−N(O) stretching.[29,30] In the spectra of the $Cr(NS)L_5^z$ complexes a band around 16 500 cm$^{-1}$ regardless of the nature of L, is seen. Furthermore, this band displays in all the thionitrosyl complexes a vibrational progression (although only weakly resolved for L = dmso) even in solution at room temperature, and it has accordingly been assigned as a $2e(d_{yz,zx},\pi^*_{NS})^* \leftarrow 1e(d_{yz,zx},\pi^*_{NS})$ transition.[7] The peak separation is 349 and 369 cm$^{-1}$ for L = $H_2O$ and $CN^-$, respectively, reflecting the Cr−N(S)

(23) It should be noted that the ADF and ORCA programs use slightly different formalisms. ADF employ Slater-type orbitals (STOs) as basis sets, whereas ORCA uses Gaussian-type orbitals (GTOs). Even though little deviation is expected between the two different formalisms when comparable basis sets are used, the differences have always been investigated explicitly and found to be small.

(24) Reed, A. E.; Curtiss, L. A.; Weinhold, F. *Chem. Rev.* **1988**, *88*, 899–926.
(25) Reed, A. E.; Weinstock, R. B.; Weinhold, F. *Chem. Rev.* **1985**, *83*, 735–746.
(26) Carpenter, J. E.; Weinhold, F. *THEOCHEM* **1988**, *46*, 41–62.
(27) TurboMole basis set library under ftp.chemie.uni-karlsruhe.de/pub/basen.
(28) Dethlefsen, J. W.; Døssing, A.; Kadziola, A. *Inorg. Chim. Acta* **2009**, *362*, 1585–1590.
(29) Manoharan, P. T.; Gray, H. B. *Inorg. Chem.* **1966**, *5*, 823–839.
(30) Kobayashi, H.; Tsujikawa, I.; Mori, M.; Yamamoto, Y. *Bull. Chem. Soc. Jpn.* **1969**, *42*, 709–715.

**Table 1.** Observed Transition Energies (in $cm^{-1}$) in the Complexes $Cr(NE)L_5^z$ with Assignments and with Calculated Values in Parentheses

| | $d_{xy} \leftarrow 1e(d_{yz,zx},\pi^*_{NE})$ | $d_{x^2-y^2} \leftarrow d_{xy}$ | $2e(d_{yz,zx},\pi^*_{NE})^* \leftarrow 1e(d_{yz,zx},\pi^*_{NE})$ | $2e(d_{yz,zx},\pi^*_{NE})^* \leftarrow d_{xy}$ | band(s) not assigned |
|---|---|---|---|---|---|
| $Cr(NO)(H_2O)_5^{2+}$ | 14 600 (14 189) | 17 800 (17 129) | 22 300 (21 048, 21 334) | 30 800 (29 067, 29954) | |
| $Cr(NS)(H_2O)_5^{2+}$ | (11 882) | (17 950) | 16 728,[a] 17 077[a] (16 686, 16 920) | 23 800 (24 293, 25 184) | 30 000 |
| $Cr(NO)(dmso)_5^{2+}$ | 13 600 | 17 600 | 22 200 | | 24 200, 29 700 |
| $Cr(NS)(dmso)_5^{2+}$ | | | 16 100 | | 22 400 |
| $Cr(NO)(nmf)_5^{2+}$ | | 17 200 | 25 300 | | |
| $Cr(NS)(nmf)_5^{2+}$ | | | 16 300 | | 20 500 |
| $Cr(NO)(CH_3CN)_5^{2+}$ | 13 400 | | 22 900 | | 31 900 |
| $Cr(NS)(CH_3CN)_5^{2+}$ | 11 500 | | 16 391,[a] 16 824,[a] 17 218[a] | | 22 500, 31 100 |
| $Cr(NO)(CN)_5^{3-}$ | 14 600 | | 22 000 | | |
| $Cr(NS)(CN)_5^{3-}$ | 13 500 | | 16 667,[a] 17 036[a] | | 24 300 |

[a] Vibronic structure.

stretching frequency in the electronically excited state. For comparison peak separations of 394 and 433 $cm^{-1}$ were found for L = $CH_3CN$.[7] These assignments are supported by DFT calculations (vide infra). The energy gap between the $1e(d_{yz,zx},\pi^*_{NS})$ and $2e(d_{yz,zx},\pi^*_{NS})^*$ orbitals is thus much lower than the energy gap between the $1e(d_{yz,zx},\pi^*_{NO})$ and $2e(d_{yz,zx},\pi^*_{NO})^*$ orbitals. Since this energy gap is a measure of the $\pi$ acidity of the ligand, it can be concluded that the NS ligand is a weaker $\pi$ acceptor than the NO ligand. The value of lowest energy transition in the complex $Cr(NO)(CN)_5^{3-}$ (in dmso solution) of 14 600 $cm^{-1}$ differs from the value reported by Gray (13 700 $cm^{-1}$),[29] whereas the energy of the second band is similar. We ascribe this to a medium effect, since the spectrum reported by Gray is recorded in aqueous solution. The isotropic EPR parameters we obtained from equilibriated dmso solutions of $Cr(NO)(CN)_5^{3-}$ at 298 K are identical to those reported earlier.[31−33] Furthermore, we can rule out the possible presence of *trans*-$Cr(NE)(dmso)(CN)_4^{2-}$ to a significant extent, since we are able to obtain values of $A_{iso}(^{13}C_{ax})$ for E = O and S from the EPR spectra of the equilibrated solutions. A more detailed discussion of the absorption spectra will be given in the sections below.

The EPR spectra of the $S = 1/2$ complexes $Cr(NS)(dmso)_5^{2+}$ and $Cr(NS)(CN)_5^{3-}$ in solution (298 K) and frozen glass (66 K) are shown in Figures 2−4. The spectra of $Cr(NS)(nmf)_5^{2+}$ and $Cr(NO)(nmf)_5^{2+}$ resemble those of the dmso complexes. Superhyperfine coupling to $^{14}N$ ($I = 1$) gives at 298 K the intense three line splitting in the complexes as seen in Figures 2 and 3 with additional low intensity lines coming from the hyperfine coupling to $^{53}Cr$ ($I = 3/2$, 9.5% natural abundance). In Figure 4, additional lines coming from superhyperfine coupling to $^{13}C$ ($I = 1/2$, enriched to 99%) are seen in the solution spectra of $Cr(NE)(^{13}CN)_5^{3-}$ (E = O, S). Simulation of the room temperature spectra gave the values for the isotropic parameters $g_{iso}$ and $A_{iso}$ listed in Tables 2−5. For comparison EPR parameters for other complexes are listed as well. The EPR spectra of $Cr(NO)(CH_3CN)_5^{2+}$ and $Cr(NS)(CH_3CN)_5^{2+}$ in $CH_3CN$ at 298 K consist of a broad band located at $g = 1.98$ without structure due to superhyperfine coupling to $^{14}N$ in the $CH_3CN$ ligands. From the frozen glass spectra, values of the anisotropic parameters $A_\perp$, $A_\parallel$, $g_\perp$, and $g_\parallel$ were obtained (Tables 2−4). It is

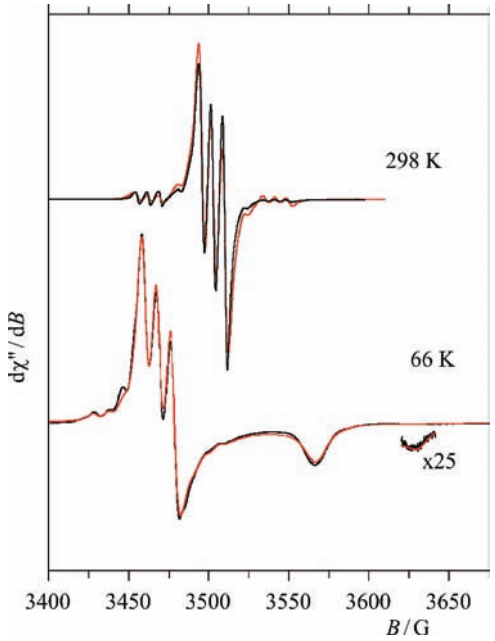


**Figure 2.** Experimental (black) and simulated (red) EPR spectra of $Cr(NS)(dmso)_5^{2+}$ at 298 and 66 K.

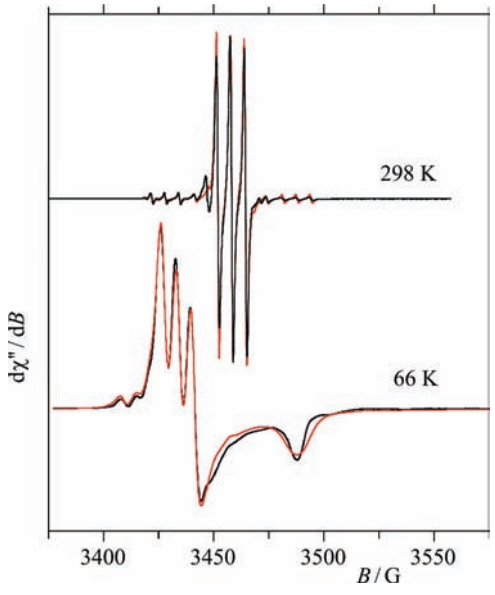


**Figure 3.** Experimental (black) and simulated (red) EPR spectra of $Cr(NS)(CN)_5^{3-}$ at 298 and 66 K.

notable that for a given L the values of $A$ for the NS and NO complexes are quite similar. This is not surprising

(31) Levina, A.; Turner, P.; Lay, P. *Inorg. Chem.* **2003**, *42*, 5392–5398.
(32) Goodman, B. A.; Raynor, J. B.; Symons, C. R. *J. Chem. Soc. A* **1968**, 1973–1977.
(33) Kuska, H. A.; Rogers, T. *J. Chem. Phys.* **1965**, *42*, 3034–3039.

given the fact that the values of $A$ reflect the ground state properties of the complex. The unpaired electron resides in the ground state in the NO and NS complexes in the $d_{xy}$ orbital (vide infra), which is not involved in bonding to the NO or NS ligand. That superhyperfine coupling to $^{14}N$ is observed at all is due to a spin−orbit coupling matrix element between the $d_{xy}$ and the $\{d_{yz}, d_{zx}\}$ set of orbitals.[34] There is, however, a tendency that the values of $A$ in a given NS complex are slightly higher than in the analogous NO complex. The DFT calculations described below reproduce this result. Concerning the values of $A_\perp(^{53}Cr)$ and $A_\parallel(^{53}Cr)$, it is relevant to discuss the parameter $P$ that describes the metal hyperfine interaction (eq 1):[35]

$$P = g_e g_N \beta_N \beta_e / \langle r^3 \rangle \quad (1)$$

Here $r$ is separation between the unpaired electron and the metal nucleus, and the other symbols have their ususal meanings. The value of $P$ can along with the value of $\kappa$ be obtained from the EPR parameters listed in Tables 2 and 3 and from eqs 2 and 3:[35]

$$A_\parallel(^{53}Cr) = P[-\kappa - (4/7) + (g_\parallel - g_e) + (3/7)(g_\perp - g_e)] \quad (2)$$

$$A_\perp(^{53}Cr) = P[-\kappa + (2/7) + (11/14)(g_\perp - g_e)] \quad (3)$$

Here the dimensionless constant $\kappa$ is often referred to as the isotropic contact parameter or Fermi contact parameter.[35] The calculated values of $P$ and $\kappa$ in the nitrosyl and thionitrosyl complexes are listed in Table 3. The free-ion values of $P$ in chromium depend on the formal oxidation state of the chromium species with $P$ decreasing almost linearly from $-24.5 \times 10^{-4}$ cm$^{-1}$ to $-50.6 \times 10^{-4}$ cm$^{-1}$ on going from chromium(0) to chromium(V).[36] Furthermore, the value of $P$ is reduced in coordination complexes. As an example to show this the value of $P$ in the chromium(V) complex $CrOCl_5^{2-}$ has been found to be $P = -35.5 \times 10^{-4}$ cm$^{-1}$.[37] This is a result of orbital expanding (larger $r$) and is often referred to as the nephelauxetic effect. In other words, the lower

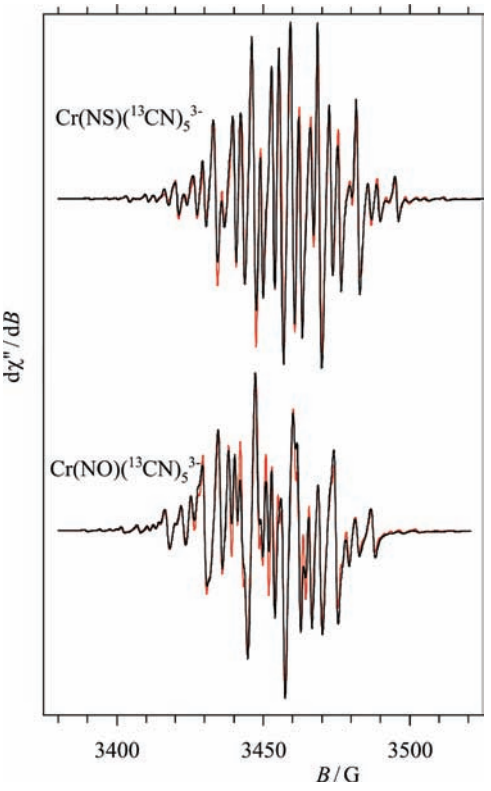


**Figure 4.** Experimental (black) and simulated (red) EPR spectra of $Cr(NE)(^{13}CN)_5^{3-}$ (E = O, S) at 298 K.

**Table 2.** Experimental Values of the EPR Parameters $g$

| | $g_{iso}$ | $g_\perp$ | $g_\parallel$ | $\Delta g_\perp$ | $\Delta g_\parallel$ | ref |
|---|---|---|---|---|---|---|
| $Cr(NO)(H_2O)_5^{2+}$ | 1.96740 | 1.994095(3) | 1.91741(2) | 0.0082 | 0.0849 | 7 |
| $Cr(NS)(H_2O)_5^{2+}$ | 1.96515 | 1.986860(8) | 1.92686(5) | 0.0154 | 0.0754 | 7 |
| $Cr(NO)(dmso)_5^{2+}$ | 1.96725 | 1.992763(2) | 1.91881(4) | 0.0095 | 0.0835 | 28 |
| $Cr(NS)(dmso)_5^{2+}$ | 1.96531 | 1.985287(3) | 1.93053(4) | 0.017 | 0.0718 | *a* |
| $Cr(NO)(nmf)_5^{2+}$ | 1.96976 | 1.99451 | 1.92380(8) | 0.0078 | 0.0785 | *a* |
| $Cr(NS)(nmf)_5^{2+}$ | 1.96730 | 1.98673 | 1.93272(9) | 0.0156 | 0.0696 | *a* |
| $Cr(NO)(CN)_5^{3-}$ | 1.99404 | 2.00513(2) | 1.9743 | −0.0028 | 0.028 | *a* |
| $Cr(NS)(CN)_5^{3-}$ | 1.99075 | 1.9998 | 1.97555 | 0.0025 | 0.0268 | *a* |

[a] This work.

**Table 4.** Experimental Values of the EPR Parameters $A(^{14}N)$

| | $A_{iso}(^{14}N)$/ $10^{-4}$cm$^{-1}$ | $A_\perp(^{14}N)$/ $10^{-4}$cm$^{-1}$ | $A_\parallel(^{14}N)$/ $10^{-4}$cm$^{-1}$ | ref. |
|---|---|---|---|---|
| $Cr(NO)(H_2O)_5^{2+}$ | 5.7 | 7.364(4) | 2.4 | 7 |
| $Cr(NS)(H_2O)_5^{2+}$ | 6.5 | 8.346(12) | 2.8 | 7 |
| $Cr(NO)(dmso)_5^{2+}$ | 5.9 | 7.540(4) | 2.6 | 28 |
| $Cr(NS)(dmso)_5^{2+}$ | 6.6 | 8.297(5) | 3.2 | *a* |
| $Cr(NO)(nmf)_5^{2+}$ | 5.7 | 7.627(11) | 1.8 | *a* |
| $Cr(NS)(nmf)_5^{2+}$ | 6.5 | 8.428(13) | 2.6 | *a* |
| $Cr(NO)(CN)_5^{3-}$ | 5.02 | 6.13(3) | 2.8 | *a* |
| $Cr(NS)(CN)_5^{3-}$ | 5.85 | 7.17(3) | 3.2 | *a* |

[a] This work.

**Table 5.** Experimental Values of the EPR Parameters $A(^{13}C)$

| | $A_{iso}(^{13}C_{eq})/10^{-4}$cm$^{-1}$ | $A_{iso}(^{13}C_{ax})/10^{-4}$cm$^{-1}$ |
|---|---|---|
| $Cr(NO)(CN)_5^{3-}$ | 11.8 | 8.1 |
| $Cr(NS)(CN)_5^{3-}$ | 12.35 | 8.65 |

**Table 3.** Experimental Values of the EPR Parameters $A(^{53}Cr)$ and Calculated Values of $P$ and $\kappa$

| | $A_{iso}(^{53}Cr)/10^{-4}$cm$^{-1}$ | $A_\perp(^{53}Cr)/10^{-4}$cm$^{-1}$ | $A_\parallel(^{53}Cr)/10^{-4}$cm$^{-1}$ | $P/10^{-4}$cm$^{-1}$ | $\kappa$ | ref |
|---|---|---|---|---|---|---|
| $Cr(NO)(H_2O)_5^{2+}$ | 23.4 | 16.0 | 38 | −23.4 | 0.96 | 7 |
| $Cr(NS)(H_2O)_5^{2+}$ | 25.3 | 18.5 | 38 | −21.0 | 1.15 | 7 |
| $Cr(NO)(dmso)_5^{2+}$ | 22.8 | 15.8 | 39 | −24.7 | 0.92 | 28 |
| $Cr(NS)(dmso)_5^{2+}$ | 24.5 | 18.5 | 38 | −21.1 | 1.15 | *a* |
| $Cr(NO)(nmf)_5^{2+}$ | 22.7 | 15.4 | 37.5 | −23.7 | 0.93 | *a* |
| $Cr(NS)(nmf)_5^{2+}$ | 24.5 | 18.5 | 37 | −20.9 | 1.19 | *a* |
| $Cr(NO)(CN)_5^{3-}$ | 17.3 | 11.3 | 29 | −19.9 | 0.85 | *a* |
| $Cr(NS)(CN)_5^{3-}$ | 18.5 | 12.5 | 31 | −20.9 | 0.88 | *a* |

[a] This work.

**Table 6.** Calculated Geometrical Parameters, Vibrational Frequencies, and Löwdin Bond Order in $Cr(N)(H_2O)_5^{2+}$ and $Cr(NE)(H_2O)_5^{2+}$ (E = O, S, Se)[a]

| | $Cr(N)(H_2O)_5^{2+}$ | $Cr(NO)(H_2O)_5^{2+}$ | $Cr(NS)(H_2O)_5^{2+}$ | $Cr(NSe)(H_2O)_5^{2+}$ |
|---|---|---|---|---|
| $d$(Cr−N)/Å | 1.552 | 1.688 (1.6969) | 1.679 | 1.691 |
| $d$(N−E)/Å | | 1.217 (1.1841) | 1.615 | 1.716 |
| $d$(Cr−$(OH_2)_{eq}$)/Å | 2.031 | 2.049 (2.012) | 2.020 | 2.049 |
| $d$(Cr−$(OH_2)_{ax}$)/Å | 2.290 | 2.088 (2.0177) | 2.098 | 2.125 |
| <(Cr−N−E)/deg | | 180.00 (179.80) | 180.00 | 180.00 |
| $\nu$(Cr−N)/$cm^{-1}$ | 1103 | 603 (602) | 728 | 421 |
| $\nu$(N−E)/$cm^{-1}$ | | 1629 (1733) | 1215 | 1110 |
| Cr−N bond order | 3.56 | 2.10 | 2.06 | 2.01 |
| N−E bond order | | 2.57 | 2.36 | 2.33 |

[a] Experimental values in parentheses, ref 8.

value of $|P|$ the higher is the covalency in the metal−ligand bonds. The oxidation state ambiguity in the nitrosyl and thionitrosyl complexes makes, however, a comparison with the free-ion values less relevant. It is clear that covalency is higher for the cyano complexes than for the other complexes. The nature of the bonding in various nitrosyl complexes has, however, earlier[32] been discussed thoroughly, and we will focus on the differences between the nitrosyl and the thionitrosyl complexes. For L = $H_2O$, dmso, and nmf it is seen that the value of $|P|$ in the thionitrosyl complexes is 85−90% of the value in the analogous nitrosyl complexes, and the covalency of the metal−ligand bonds in the thionitrosyl complexes is accordingly slightly higher than in the nitrosyl complexes. For the three complexes the values of $(P_{NO}/P_{NS})^{1/3} = (\langle r_{NS}^3\rangle/\langle r_{NO}^3\rangle)^{1/3}$ lie in the range 1.03−1.05 meaning that the d orbital has expanded 3−5% on going from the nitrosyl ligand to the thionitrosyl ligand. The covalency of the bonds in the two cyano complexes are similar to each other. The Fermi contact parameter $\kappa$ expresses the contribution to the hyperfine interaction from the unpaired electron at the nucleus, which is only possible for s electrons. The nonvanishing values for $\kappa$ show that unpaired electron has some s electron character. This can be explained in terms of polarization of inner s electrons resulting from interaction with the unpaired 3d electron through configuration interaction.[36] In Table 3 it is seen that for L = $H_2O$, dmso, and nmf values of $\kappa$ are found in the range 0.92−0.96 and 1.15−1.19 in the nitrosyl and thionitrosyl complexes, repectively. In this regard, it is again noted that the two cyano complexes are similar to each other but differs significantly from the other complexes.Values of $\kappa$ larger than unity are frequently observed. In a series of nitrido complexes of chromium(V) containing the $CrN^{2+}$ core, also with a $d_{xy}^1$ ground state electron configuration, values of $\kappa$ were found in the range 1.11−1.42.[38] Previous work[38,39] suggests that $\kappa$ might increase with a decrease in $|P|$, and it seems to be case in the present work. The values of $g$ are reflected by the excited state energies, and the different spectrochemical properties between the NS and NO ligand should accordingly be reflected in the values of $g$. The key parameter is the shift $\Delta g$ from the free electron value $g_e = 2.002319$ as expressed in eqs 4 and 5:[34]

$$\Delta g_\perp = 2.002319 - g_\perp = 2\zeta/\Delta E[2e(d_{yz,zx}, \pi^*_{NE})^* - d_{xy}] \quad (4)$$

$$\Delta g_\parallel = 2.002319 - g_\parallel = 8\zeta/\Delta E(d_{x^2-y^2} - d_{xy}) \quad (5)$$

Here $\zeta$ is the single spin−orbit coupling parameter. The free-ion value of $\zeta$ in chromium depends on the formal oxidation state, and the value increases almost linearly from 135 $cm^{-1}$ to 380 $cm^{-1}$ on going from chromium(I) to chromium(V).[36] An inspection of the values of $\Delta g$ listed in Table 2 shows that for L = $H_2O$, dmso, and nmf, the value of $\Delta g_\perp$ for the NS complex is about twice the value in the NO complex in accordance with the fact that the energy of the $2e(d_{yz,zx},\pi^*_{NS})^*$ orbital is lower than the $2e(d_{yz,zx},\pi^*_{NO})^*$ orbital (vide supra). The DFT calculations outlined below address this point in more detail. Regarding $\Delta g_\parallel$ it is seen that the value of $\Delta g_\parallel$ in the thionitrosyl complexes is 86−89% of the value in the analogous nitrosyl complexes for L = $H_2O$, dmso, and nmf. If we assume that the energy difference $\Delta E(d_{x^2-y^2} - d_{xy})$ for a given L has the same value (vide supra), the lower value of $\Delta g_\parallel$ should consequently be caused by a lower value of $\zeta$ in the thionitrosyl complexes ($\zeta_{NS}$) than in the nitrosyl complexes ($\zeta_{NO}$) with the ratio $\zeta_{NS}/\zeta_{NO}$ lying in the range 0.86−0.89. This is in accordance with the above-mentioned fact that the value of $|P|$ in the thionitrosyl complexes is 85−90% of the value in the analogous nitrosyl complexes.

**DFT Calculations. Geometry.** The relevant optimized, geometrical parameters and vibrational stretching frequencies for the $Cr(X)(H_2O)_5^{2+}$ complexes are compiled in Table 6. Only the $Cr(NO)(H_2O)_5^{2+}$ complex has been characterized by means of X-ray diffraction,[8,40] and the calculated parameters fit the experimental values well. In the crystal structure determined by Ardon,[40] a Cr−$(OH_2)_{ax}$ distance of 2.057(2) Å was found. This shows that hydrogen bonding and packing forces might have a small influence on the bond distances. The values for the nitrido and thionitrosyl complexes lie within the experimentally determined values for similar compounds.[4,41] The calculated value of $\nu_{NS}$ in $Cr(NS)(H_2O)_5^{2+}$ is close to the experimentally determined in $Cr(NS)(dmso)_5^{2+}$ ($\nu_{NS}$ = 1265 $cm^{-1}$). The only selenonitrosyl complex reported[42]

(34) Azuma, N.; Imori, Y.; Yoshida, H.; Tajima, K.; Li, Y.; Yamauchi, J. *Inorg. Chim. Acta* **1997**, *266*, 29–36.
(35) McGarvey, B. R. *Transition Met. Chem.* **1966**, *3*, 89–201.
(36) Mabbs, F. E.; Collison, D. *Electron Paramagnetic Resonance of d Transition Metal Compounds*; Elsevier: New York, 1992.
(37) Kon, H.; Sharpless, N. E. *J. Chem. Phys.* **1965**, *42*, 906–909.
(38) Hori, A.; Ozawa, T.; Yoshida, Y.; Imori, Y.; Kuribayashi, Y.; Nakano, E.; Azuma, N. *Inorg. Chim. Acta.* **1998**, *281*, 207–213.
(39) Azuma, N.; Ozawa, T.; Tsuboyama, S. *J. Chem. Soc., Dalton Trans.* **1994**, 2609–2613.
(40) Ardon, M.; Cohen, S. *Inorg. Chem.* **1993**, *32*, 3241–3243.
(41) Birk, T.; Bendix, J. *Inorg. Chem.* **2003**, *42*, 7608–7615.
(42) Crevier, T. J.; Lovell, S.; Mayer, J. M.; Rheingold, A. L.; Guzei, I. A. *J. Am. Chem. Soc.* **1998**, *120*, 6607–6608.

**Table 7.** Atomic Charges Obtained by Mulliken, Löwdin, and NPA Analyses

| | Cr | N | E | $O_{eq}$ | $O_{ax}$ |
|---|---|---|---|---|---|
| | | | Mulliken | | |
| $Cr(N)(H_2O)_5^{2+}$ | +0.825 | −0.302 | | −0.271 | −0.357 |
| $Cr(NO)(H_2O)_5^{2+}$ | +0.701 | −0.107 | −0.092 | −0.275 | −0.292 |
| $Cr(NS)(H_2O)_5^{2+}$ | +0.760 | −0.443 | +0.220 | −0.284 | −0.311 |
| $Cr(NSe)(H_2O)_5^{2+}$ | +0.759 | −0.520 | +0.340 | −0.279 | −0.301 |
| | | | Löwdin | | |
| $Cr(N)(H_2O)_5^{2+}$ | +0.367 | −0.017 | | +.0417 | +0.335 |
| $Cr(NO)(H_2O)_5^{2+}$ | +0.315 | −0.101 | +0.145 | +0.409 | +0.385 |
| $Cr(NS)(H_2O)_5^{2+}$ | +0.306 | −0.350 | +0.407 | +0.390 | +0.355 |
| $Cr(NSe)(H_2O)_5^{2+}$ | +0.324 | −0.343 | +0.430 | +0.408 | +0.374 |
| | | | NPA | | |
| $Cr(N)(H_2O)_5^{2+}$ | +0.808 | +0.077 | | −0.841 | −0.954 |
| $Cr(NO)(H_2O)_5^{2+}$ | +0.708 | +0.253 | −0.096 | −0.844 | −0.896 |
| $Cr(NS)(H_2O)_5^{2+}$ | +0.776 | −0.425 | +0.501 | −0.841 | −0.908 |
| $Cr(NSe)(H_2O)_5^{2+}$ | +0.805 | −0.537 | +0.619 | −0.840 | −0.903 |

is Os(NSe)(tp)$Cl_2$ where tp = hydridotris(1-pyrazolylborate) with an N−Se distance of 1.629(10) Å, < Os−N−Se = 164.7(6)°, and $\nu_{NSe}$ = 1156 $cm^{-1}$ close to the calculated values in $Cr(NSe)(H_2O)_5^{2+}$. The $Cr-(OH_2)_{eq}$ distance in the four complexes is the same, lying in the range 2.020−2.049 Å. This similarity will be discussed under the population analyses. The $Cr-(OH_2)_{eq}$ is seen to be in between the $Cr-(OH_2)$ distance of 1.958(4) Å found in $[Cr(H_2O)_6](NO_3)_3 \cdot 3H_2O$[43a] and the $Cr-(OH_2)_{eq}$ distance of 2.065 Å in $(NH_4)_2Cr(H_2O)_6(SO_4)_2$.[43b] The three NE complexes contain a linear Cr−N−E core with Cr−N distances that are identical within 0.01 Å. The nitrido ligand is seen to exhibit a strong *trans* influence, in contrast to the three NE ligands, with an elongation of the $Cr-(OH_2)_{ax}$ distance of 0.26 Å. It should be noted that the Cr−N bond in the NE complexes is only 0.15 Å longer than in the nitrido complex. The calculated bond orders fall from 3.5 in the nitrido complex to around 2 in $Cr(NE)(H_2O)_5^{2+}$. Thus, although significant multiple bond character is present in the NE series, the nitrido bond order is predicted higher.

**DFT Calculations. Charge and Population Analyses.** The charges for Cr, N, E, and O are compiled in Table 7; as expected, the charge analyses yield different numerical results, but the trends are comparable. Two trends deserve a comment. *First*, all analyses agree that the equatorial oxygen charges are similar for the whole $Cr(X)(H_2O)_5^{2+}$ series, indicating that the electronic structure in the equatorial plane does not change significantly through the series in agreement with the similar $Cr-(OH_2)_{eq}$ distances. Furthermore, the axial oxygen charge is similar for the NE complexes but differs noticeably from the nitrido complex, also in line with the observed *trans* influence from the nitrido ligand. *Second*, the chromium charge is the highest for the nitrido complex and the lowest for the nitrosyl complex with the thio- and selenonitrosyl being similar and between the other two.

When proceeding to the nitrogen charges, the picture becomes blurred. This is mainly due to the nitrido complex whose nitrogen charge is difficult to relate to the remaining series. However, it is evident that none of the analyses confirm a formal charge of −3 on the nitrido ligand. Within the series $Cr(NE)(H_2O)_5^{2+}$, the nitrogen charge becomes increasingly negative in the series NO < NS ≈ NSe, thus confirming the higher electron density on the nitrogen atom in NS than on the nitrogen atom in NO in the uncoordinated NE molecules. The $\sigma$ donor strength of the ligands is not reflected by the charge analyses, but the Löwdin population analysis (see Supporting Information Table S-5) shows that while the $a_1(d_{z^2})$ orbital in the nitrido complex consists of equal amounts of $Cr(d_{z^2})$ and $N(p_z)$ orbitals, there is no contribution from the $N(p_z)$ orbitals to the $a_1(d_{z^2})$ orbitals in the NE complexes. The nitrido ligand is thus a stronger $\sigma$ donor than the three NE ligands because of the significantly enhanced covalent contributions to the $a_1(d_{z^2})$ orbital. Earlier studies[10] seem to have ignored the significant increase in $\sigma$ donor strength in their comparison of complexes $Mn(N)(CN)_5^{3-}$ versus $Mn(NO)(CN)_5^{3-}$ related to the series investigated here. The studies of $Mn(N)(CN)_5^{3-}$ and $Mn(NO)(CN)_5^{3-}$ showed that the $2e \leftarrow d_{xy}$ transitions were of similar energies, and we also find that $Cr(NO)(H_2O)_5^{2+}$, $Cr(NS)(H_2O)_5^{2+}$, and $Cr(NSe)(H_2O)_5^{2+}$ have $2e \leftarrow d_{xy}$ transitions which compare well with $Cr(N)(H_2O)_5^{2+}$; the transition energy in $Cr(NO)(H_2O)_5^{2+}$ is even slightly higher. So far the conclusions from ref 11 can be extended to include the whole series studied here. However, the fact that orbital populations (Supporting Information Table S-5) show that the nitrido complex $Cr(N)(H_2O)_5^{2+}$ have 2e orbitals with a higher d orbital character than in the complexes $Cr(NO)(H_2O)_5^{2+}$, $Cr(NS)(H_2O)_5^{2+}$, and $Cr(NSe)(H_2O)_5^{2+}$ shows that the electronic structure of $Cr(N)(H_2O)_5^{2+}$ differs significantly from the three other complexes. Spin populations (compiled in Table 8) generally show an NE ligand of increasing radical character through the series NO < NS < NSe. The change is almost exclusively mediated by the chalcogen atom. Problems with spin contamination were also most significant for the heavier chalcogen atoms (see Supporting Information Table S-6).

**Table 8.** Spin Populations Obtained from Mulliken and Löwdin Analyses

| | Cr | N | E |
|---|---|---|---|
| | | Mulliken | |
| $Cr(N)(H_2O)_5^{2+}$ | +1.40 | −0.38 | |
| $Cr(NO)(H_2O)_5^{2+}$ | +1.50 | −0.23 | −0.21 |
| $Cr(NS)(H_2O)_5^{2+}$ | +1.70 | −0.22 | −0.42 |
| $Cr(NSe)(H_2O)_5^{2+}$ | +1.78 | −0.23 | −0.49 |
| | | Löwdin | |
| $Cr(N)(H_2O)_5^{2+}$ | +1.28 | −0.33 | |
| $Cr(NO)(H_2O)_5^{2+}$ | +1.38 | −0.20 | −0.20 |
| $Cr(NS)(H_2O)_5^{2+}$ | +1.55 | −0.19 | −0.40 |
| $Cr(NSe)(H_2O)_5^{2+}$ | +1.63 | −0.19 | −0.47 |

**DFT Calculations. Electronic Structures.** For each NE complex, there are seven pairs of spin orbitals with 3d metal and $\pi^*$(NE) character stemming from interactions between the five 3d orbitals on the chromium atom and the two $\pi^*$ orbitals on the NE ligand. For the nitrido complex, there are only five pairs of spin orbitals with a high degree of 3d character, since the nitrido ligand as a pure $\sigma$ and $\pi$ donor does not accept electron density from the metal ion. The orbital energies are compiled in

(43) (a) Lazar, D.; Ribar, B.; Divjakovic, V.; Meszaros, C. *Acta Crystallogr.* **1991**, *C47*, 1060–1062. (b) Dobe, C.; Noble, C.; Carver, G.; Tregenna-Piggot, P. L. W.; McIntyre, G. J.; Barra, A.-L.; Neels, A.; Juranyi, F. *J. Am. Chem. Soc.* **2004**, *126*, 16639–16652.

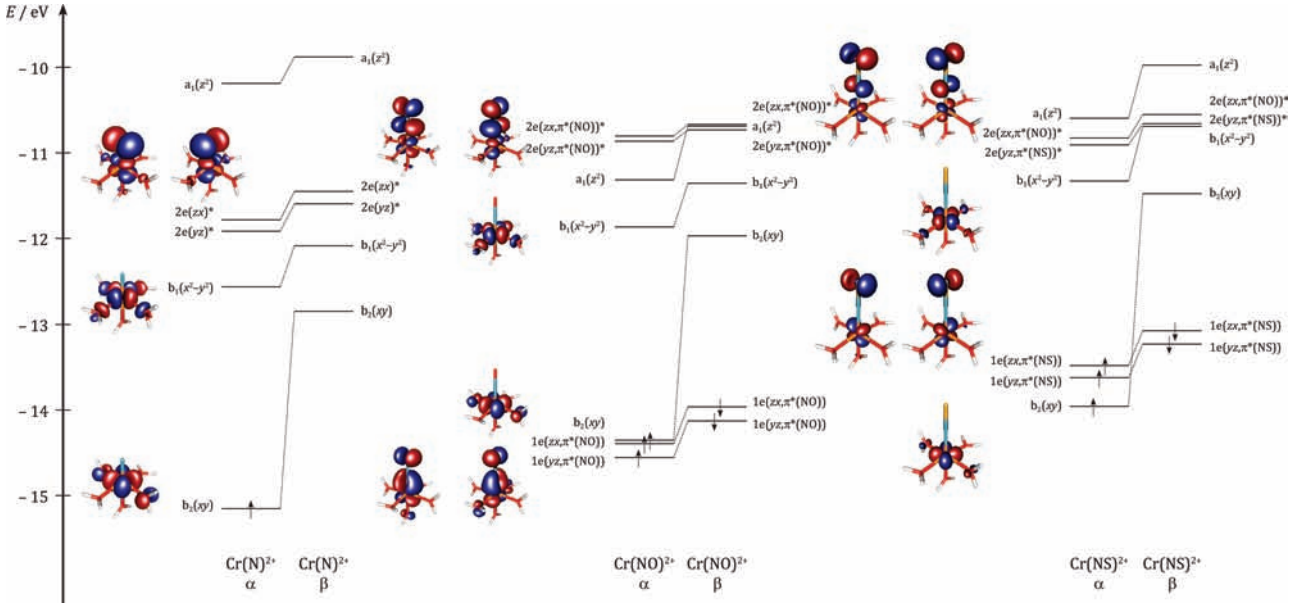


**Figure 5.** Molecular orbital diagrams with representations of some α spin orbitals. The $\beta$ spin orbitals are qualitatively identical. The $a_1(d_{z^2})$ orbital is not easily recognized and because of lack of space not shown. The orbital diagram of the NSe complex resembles the orbital diagram of the NS complex and is thus omitted.

Supporting Information Table S-4, and orbital diagrams with contour plots of some orbitals are shown in Figure 5. The orbitals are labeled in accordance with an idealized $C_{4v}$ symmetry even though this can never be the case with an axial water ligand. This choice results in a non-degenerate e set of orbitals, but we prefer the wrong labeling to be in accordance with earlier studies on the electronic structure of nitrido and nitrosyl complexes.[29−32]

Calculations with spin-restricted, localized orbitals[44] (Figure 6) confirm that the unpaired electron is in a $d_{xy}$ metal-based orbital for all applied functionals (BP86, BLYP and B3LYP), which is in accordance with an older study by Shim et al.[45] Here, we arbitrarily label the α block as the block with "excess" spin. Thus, excitations *from* the $d_{xy}$ orbital will only be considered within the α block (where it is occupied) whereas transitions *to* the $d_{xy}$ orbital will only be considered within the $\beta$ block (where it is empty).

From the MO diagram in Figure 5, the most striking qualitative difference between the complexes is seen to be the position of the $a_1(d_{z^2})$ orbital. In the $Cr(N)^{2+}$ complex, the very short Cr−N bond of course results in a very high energy of this orbital. Functionalization of the nitrido ligand has a profound effect on this orbital and it drops below the $2e(d_{yz,zx},\pi^*_{NO})^*$ set in the nitrosyl complex. The $a_1(d_{z^2})$ orbital remains above the $2e(d_{yz,zx},\pi^*_{NE})^*$ orbitals for the NS and NSe complexes. The position of the $a_1(d_{z^2})$ and $2e(d_{yz,zx},\pi^*_{NE})^*$ orbitals is consistent with the slightly larger $\sigma$ donor strength for NS and NSe accompanied by weaker $\pi$ interactions for these to ligands (vide infra).

Orbital energy differences and excitation energies (from TDDFT) have been calculated and listed in Table 9 (see Supporting Information Tables S-1, S-2, and S-3 for further calculations). TDDFT has shown to be a powerful computational tool in predictions of electronic transitions in organic and transition metal compounds. However, there are several well-known pitfalls, most notably the following: (1) Charge transfer transition energies are often predicted much too low, (2) double excitations are not included and these will be missing, and (3) electronic relaxation is not accounted for in the excited state. The underlying causes have been discussed in detail by Neese.[46,47] Despite the mentioned pitfalls, transitions which primarily are of d-d character are usually predicted with good accuracy, see for instance the study by Grapperhaus et al.[48]

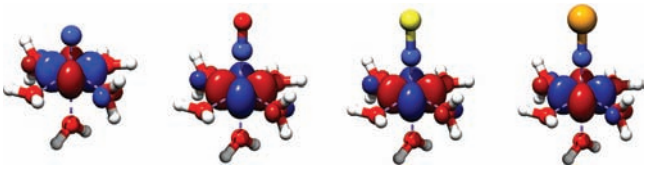

**Figure 6.** Representation of spin-restricted, localized orbitals in Cr(X)-$(H_2O)_5^{2+}$ (X = N, NO, NS, NSe). The unpaired electron is seen to be located in a $d_{xy}$ orbital in all four complexes.

The transitions between the $1e(d_{yz,zx},\pi^*_{NE})$ and $2e(d_{yz,zx},\pi^*_{NE})^*$ sets of orbitals could not be unambiguously assigned since the transitions often involve more than two states leading to a wide distribution of different energies for transitions of this origin. Some trends become clear. *First*, the transition from the $d_{xy}$ to the $d_{x^2-y^2}$ orbital in the complexes $Cr(X)(H_2O)_5^{2+}$ has an energy that is almost independent of the nature of X. This is not surprising since these orbitals are pointing out toward or out between the equatorial water ligands that are located at the same distance from the chromium center in the four complexes (vide supra). As earlier discussed by Birk and

(44) Neese, F. *J. Am. Chem. Soc.* **2006**, *128*, 10213–10222.
(45) Shim, I.; Gingerich, K. A.; Mandix, K.; Feng, X. *Inorg. Chim. Acta* **1995**, *229*, 455–460.
(46) Neese, F. *Coord. Chem. Rev.* **2009**, *253*, 526–563.
(47) Neese, F.; Petrenko, T.; Ganyushin, D.; Olbrich, G. *Coord. Chem. Rev.* **2007**, *251*, 288–327.
(48) Grapperhaus, C. A.; Bill, E.; Weyhermüller, T.; Neese, F.; Wieghardt, K. *Inorg. Chem.* **2001**, *40*, 4191–4198.

**Table 9.** Excitation Energies (in $cm^{-1}$) Obtained from TDDFT with BP86 and TZVPP and (in Parentheses) Orbital Energy Differences for $Cr(X)(H_2O)_5^{2+}$ Obtained with BP86 and TZ2P[a]

| X | $d_{x^2-y^2} \leftarrow d_{xy}$ | $d_{z^2} \leftarrow d_{xy}$ | $2e(d_{yz})^* \leftarrow d_{xy}$ | $2e(d_{zx})^* \leftarrow d_{xy}$ | $d_{xy} \leftarrow 1e(d_{yz})$ | $d_{xy} \leftarrow 1e(d_{zx})$ | $2e(d_{yz})^* \leftarrow 1e(d_{yz})$ | $2e(d_{zx})^* \leftarrow 1e(d_{zx})$ |
|---|---|---|---|---|---|---|---|---|
| N | 17 687 | 40 342 | 24 910 | 24 875 | 30 786 | 28 476 | | |
| | (20 878) | (40 078) | (26 131) | (27 195) | (31 107) | (27 291) | (39 146) | (36 389) |
| NO | 17 129 | 24 416 | 29 067 | 29 954 | 15 567 | 14 189 | *b* | *b* |
| | (20 049) | (24 522) | (28 159) | (28 629) | (17 391) | (16 062) | (29 799) | (28 950) |
| NS | 17 950 | 28 479 | 24 293 | 25 184 | 12 999 | 11 882 | *c* | *c* |
| | (21 198) | (27 112) | (24 600) | (25 239) | (14 111) | (12 870) | (21 912) | (21 401) |
| NSe | 17 095 | 27 913 | 25 396 | 26 021 | 11 734 | 11 882 | | |
| | (20 437) | (26 805) | (24 633) | (25 241) | (12 940) | (11 879) | (20 397) | (20 042) |

[a] For the energy differences, only α orbitals are considered with exception of the transitions to the $d_{xy}$ orbital, where only $\beta$ orbitals are considered. For the excitation energies calculated with TDDFT, mixing of α and $\beta$ transitions occur. [b] TDDFT yields five transition energies that can be assigned to the $2e(d_{yz,zx},\pi^*_{NO})^* \leftarrow 1e(d_{yz,zx},\pi^*_{NO})$ transition, namely, 21 048, 21 334, 25 726, 30 262, and 31 578 $cm^{-1}$. [c] TDDFT yields four transition energies that can be assigned to the $2e(d_{yz,zx},\pi^*_{NS})^* \leftarrow 1e(d_{yz,zx},\pi^*_{NS})$ transition, namely, 16 686, 16 920, 20 532, and 23 404 $cm^{-1}$.

Bendix in their studies of the nitrido chromium complexes,[41] it is relevant to compare the energy of the $d_{x^2-y^2} \leftarrow d_{xy}$ transition to the energy of the lowest energy spin-allowed transition ($^4T_2 \leftarrow {}^4A_2$, $O_h$) in the octahedral chromium(III) complex $CrL_6^z$ which is a direct measure of the ligand field splitting parameter $\Delta_o$, the one-electron energy difference between the $t_{2g}$ and $e_g$ orbitals.[49] It is notable that the TDDFT calculations give transition energies (17 095−17 950 $cm^{-1}$) close to the energy of the $^4T_2 \leftarrow {}^4A_2$ transition in $Cr(H_2O)_6^{3+}$ found to be 17 420 $cm^{-1}$.[50] This indicates that the electronic structure in the equatorial plane in $Cr(X)^{2+}$ is similar to the electronic structure in $Cr^{3+}$. *Second*, the energy of the $d_{z^2}$ orbital, and also the energy of the $d_{z^2} \leftarrow d_{xy}$ transition, is strongly dependent on the $\sigma$ donor properties of the ligand X. From the transition energies in Table 8 it is seen that $N^{3-}$ as expected is the strongest $\sigma$ donor, but it should also be noted that both NS and NSe are substantially stronger $\sigma$ donors than NO. *Third*, the transition from the $1e(d_{yz,zx},\pi^*_{NE})$ set to the $d_{xy}$ orbital, from the $d_{xy}$ orbital to the $2e(d_{yz,zx},\pi^*_{NE})$ set, and from the $1e(d_{yz,zx},\pi^*_{NE})$ to the $2e(d_{yz,zx},\pi^*_{NE})^*$ set shift to lower energy when going from NO to NS and NSe, which indicates that NS and NSe are weaker $\pi$ acceptors than NO. This is in agreement with the conclusion from the EPR spectra, that the energy of the $2e(d_{yz,zx},\pi^*_{NE})^* \leftarrow d_{xy}$ transition is lowered on going from NO to NS. The nitrido ligand should not be considered in this context, since it is not a $\pi$ acceptor.

Concerning the assignment of the optical absorption spectra of $Cr(NO)(H_2O)_5^{2+}$ and $Cr(NS)(H_2O)_5^{2+}$ (see Figure 7) a Gaussian resolution of the spectrum of $Cr(NO)(H_2O)_5^{2+}$ in the range 12 000−19 000 $cm^{-1}$ reveals the presence of a low-intensity band ($\varepsilon$ = 3.5 $M^{-1}$ $cm^{-1}$) at 14 635 $cm^{-1}$. On the basis of the discussion above and the results in Table 9, we assign this as a $d_{xy} \leftarrow 1e(d_{yz,zx},\pi^*_{NO})$ transition, and the absorption band at 17 800 $cm^{-1}$ as the $d_{x^2-y^2} \leftarrow d_{xy}$ transition, in reasonable agreement with the TDDFT calculations. In $Cr(NS)(H_2O)_5^{2+}$, the $d_{xy} \leftarrow 1e(d_{yz,zx},\pi^*_{NS})$ transition is apparently too weak to be observed and the $d_{x^2-y^2} \leftarrow d_{xy}$ transition, which also should be located around 17 800 $cm^{-1}$, is covered by the intense band that we tentatively assigned as the $2e(d_{yz,zx},\pi^*_{NS})^* \leftarrow 1e(d_{yz,zx},\pi^*_{NS})$ transition. Further, the TDDFT calculations have been used to assign some of the remaining bands in the absorption spectra of $Cr(NO)(H_2O)_5^{2+}$ and $Cr(NS)(H_2O)_5^{2+}$. In Figure 7, the $d_{xy} \leftarrow 1e(d_{yz,zx},\pi^*_{NE})$ and $2e(d_{yz,zx},\pi^*_{NE})^* \leftarrow d_{xy}$ transitions (E = O, S) have been marked along with the $d_{x^2-y^2} \leftarrow d_{xy}$ transition for $Cr(NO)(H_2O)_5^{2+}$.

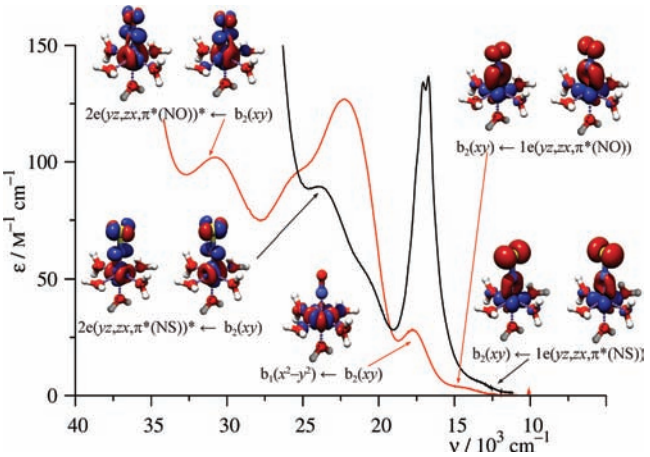


**Figure 7.** Optical absorption spectra of $Cr(NS)(H_2O)_5^{2+}$ (black) and $Cr(NO)(H_2O)_5^{2+}$ (red) with some spectral assignments. The insets are TDDFT density differences. The bands at 16 600 $cm^{-1}$ and 22 200 $cm^{-1}$ are transitions between the $1e(d_{yz,zx},\pi^*_{NE})$ and $2e(d_{yz,zx},\pi^*_{NE})^*$ sets of orbitals in $Cr(NS)(H_2O)_5^{2+}$ and $Cr(NO)(H_2O)_5^{2+}$, respectively.

As discussed above, the energies for the transitions between the $1e(d_{yz,zx},\pi^*_{NE})$ and $2e(d_{yz,zx},\pi^*_{NE})^*$ sets of orbitals cannot be unambiguously determined, since TDDFT, because of coupling of states, predicts up to five transition energies corresponding to transitions between orbitals with $d_{yz}$, $d_{zx}$, and $\pi^*_{NE}$ character. For $Cr(NO)(H_2O)_5^{2+}$, two of the calculated energies are close to the energy of the intense band around 22 000 $cm^{-1}$; for $Cr(NS)(H_2O)_5^{2+}$, two of the calculated energies are close to the energy of the intense band around 17 000 $cm^{-1}$. Accordingly, the earlier assignment[7,29] of these bands as $2e(d_{yz,zx},\pi^*_{NE})^* \leftarrow 1e(d_{yz,zx},\pi^*_{NE})$ transitions is confirmed.

Concerning a possible assignment of the spectra of the complexes with L = dmso, nmf, $CH_3CN$, and $CN^-$ it is seen in Table 1 and Figure 1 that there are several complexes with a weak absorption band in the range 11 500−14 600 $cm^{-1}$. On the basis of the discussion above we assign this band as a $d_{xy} \leftarrow 1e(d_{yz,zx},\pi^*_{NE})$ transition. For L = $CH_3CN$ and $CN^-$ it is seen that the transition energy is 1000−2000 $cm^{-1}$ lower in the thionitrosyl complex than in the analogous nitrosyl complex in agreement with the calculations of the aqua complexes (vide infra).

(49) König, E. *Struct. Bonding* (*Berlin*) **1971**, *9*, 175–212.
(50) Mønsted, L.; Mønsted, O. *Acta Chem. Scand.* **1973**, *27*, 2121–2130.

**Table 10.** Calculated (with BP86, ccpVQZ STO) Hyperfine Coupling Constants with the Experimental Values in Parentheses

| | $A_{iso}(^{53}Cr)/10^{-4}$ cm$^{-1}$ | $A_{11}(^{53}Cr)/10^{-4}$ cm$^{-1}$ | $A_{22}(^{53}Cr)/10^{-4}$ cm$^{-1}$ | $A_{33}(^{53}Cr)/10^{-4}$ cm$^{-1}$ |
|---|---|---|---|---|
| $Cr(N)(H_2O)_5^{2+}$ | 27.4 | 42.7 | 19.8 | 19.6 |
| $Cr(NO)(H_2O)_5^{2+}$ | 20.8(23.4) | 34.5(38) | 14.3(16) | 13.7(16) |
| $Cr(NS)(H_2O)_5^{2+}$ | 23.1(25.3) | 35.6(38) | 17.2(18.5) | 16.5(18.5) |
| $Cr(NSe)(H_2O)_5^{2+}$ | 25.4 | 36.6 | 20.1 | 19.3 |
| | $A_{iso}(^{14}N)/10^{-4}$ cm$^{-1}$ | $A_{11}(^{14}N)/10^{-4}$ cm$^{-1}$ | $A_{22}(^{14}N)/10^{-4}$ cm$^{-1}$ | $A_{33}(^{14}N)/10^{-4}$ cm$^{-1}$ |
| $Cr(N)(H_2O)_5^{2+}$ | −1.3 | −3.1 | −2.6 | 1.8 |
| $Cr(NO)(H_2O)_5^{2+}$ | −5.5(5.7) | −8.0(7.36) | −7.4(7.36) | −1.0(2.4) |
| $Cr(NS)(H_2O)_5^{2+}$ | −6.0(6.5) | −8.5(8.35) | −7.7(8.35) | −1.7(2.8) |
| $Cr(NSe)(H_2O)_5^{2+}$ | −5.9 | −8.4 | −7.6 | −1.7 |
| | $A_{iso}(^{17}O_x)/10^{-4}$ cm$^{-1}$ | $A_{iso}(^{17}O_y)/10^{-4}$ cm$^{-1}$ | $A_{iso}(^{17}O_z)/10^{-4}$ cm$^{-1}$ | $A_{iso}(E)/10^{-4}$ cm$^{-1}$ |
| $Cr(N)(H_2O)_5^{2+}$ | 2.95 | 2.79 | −0.99 | |
| $Cr(NO)(H_2O)_5^{2+}$ | 2.95 | 3.76 | 1.70 | 3.2 (E = $^{17}$O) |
| $Cr(NS)(H_2O)_5^{2+}$ | 2.58 | 3.77 | 1.42 | 3.2 (E = $^{33}$S) |
| $Cr(NSe)(H_2O)_5^{2+}$ | 2.22 | 3.68 | 1.40 | 33.6 (E = $^{77}$Se) |

In the $Cr(NS)(dmso)_5^{2+}$, $Cr(NO)(nmf)_5^{2+}$, and $Cr(NS)(nmf)_5^{2+}$ complexes, this transition is apparently too weak to be observed. With regard to the $d_{x^2-y^2} \leftarrow d_{xy}$ transition seen at 17 800 cm$^{-1}$ in $Cr(NO)(H_2O)_5^{2+}$, we suggest that the bands at 17 600 cm$^{-1}$ and 17 200 cm$^{-1}$ in $Cr(NO)(dmso)_5^{2+}$ and $Cr(NO)(nmf)_5^{2+}$, respectively, are $d_{x^2-y^2} \leftarrow d_{xy}$ transitions because of the relatively close proximity of the dmso and nmf to $H_2O$ in the spectrochemical series.[51] In the analogous thionitrosyl complexes we should see the $d_{x^2-y^2} \leftarrow d_{xy}$ transition at the same energy, but the intense $2e(d_{yz,zx},\pi^*_{NS})^* \leftarrow 1e(d_{yz,zx},\pi^*_{NS})$ transition around 16 500 cm$^{-1}$ covers the $d_{x^2-y^2} \leftarrow d_{xy}$ transition. The $d_{x^2-y^2} \leftarrow d_{xy}$ transition in the $CH_3CN$ and $CN^-$ complexes is shifted to higher energy and covered by other transitions. Finally, it is a general feature that the intense $2e(d_{yz,zx},\pi^*_{NE})^* \leftarrow 1e(d_{yz,zx},\pi^*_{NE})$ transitions occur at 16 000−17 000 cm$^{-1}$ in the thionitrosyl complexes and at 22 000−23 000 cm$^{-1}$ in the nitrosyl complexes.

**DFT Calculations. EPR Parameters.** The hyperfine coupling constants to $^{53}$Cr, $^{14}$N, $^{17}$O, $^{33}$S, and $^{77}$Se have been calculated for the four complexes and are compiled in Table 10. The calculated parameters fit the experimental unprecedentedly well and confirm the trend that the hyperfine coupling constants to both chromium and nitrogen in $Cr(NO)(H_2O)_5^{2+}$ and $Cr(NS)(H_2O)_5^{2+}$ are highest for the thionitrosyl complex. However, as the superhyperfine coupling constants to the oxygen atoms in the water ligands in $Cr(NS)(H_2O)_5^{2+}$ are either smaller than or essentially identical with the analogous parameters for the nitrosyl complex, the calculations do not confirm the trend observed in $Cr(NO)(CN)_5^{3-}$ and $Cr(NS)(CN)_5^{3-}$, namely, that the coupling constants to all atoms are higher for the thionitrosyl complex. We do not see this as an invalidation of the calculations as water and cyanide are indeed very different ligands. If anything, this result shows that it is not an inherent property of thionitrosyl complexes that their coupling constants are numerically larger than the nitrosyl complexes.

Upon comparing the EPR parameters for the nitrido complex with those for the NE complexes, it is evident that there are quite large differences. The common trend is that the coupling constant to chromium is largest for the nitrido complex whereas the coupling constant to nitrogen is largest for the NE complexes. An interpretation of this requires an analysis of the different contributions to the coupling constants which will be considered in a forthcoming publication.

We note that the coupling constant to selenium in $Cr(NSe)(H_2O)_5^{2+}$ is $33.56 \times 10^{-4}$ cm$^{-1}$. The magnitude of this value could invalidate the whole calculation for the selenonitrosyl complex were it not for the fact that the rest of the coupling constants are reasonable.

## Summary

The DFT studies of the series of $S = 1/2$ complexes $Cr(N)(H_2O)_5^{2+}$, $Cr(NO)(H_2O)_5^{2+}$, $Cr(NS)(H_2O)_5^{2+}$, and $Cr(NSe)(H_2O)_5^{2+}$ show that the unpaired electron resides in a metal-based $d_{xy}$ orbital. The fact that the $Cr-(OH_2)_{eq}$ distance, the equatorial oxygen charges, and the energy of the $d_{x^2-y^2} \leftarrow d_{xy}$ transition is similar for the whole series show that the electronic structure in the equatorial plane is very similar in all four complexes. The energy of the $d_{x^2-y^2} \leftarrow d_{xy}$ transition in the complex $Cr(NO)(H_2O)_5^{2+}$ (calc. 17 100 cm$^{-1}$, exp. 17 800 cm$^{-1}$) is close to the energy of the $^4T_2 \leftarrow {}^4A_2$ transition in $Cr(H_2O)_6^{3+}$. The $\sigma$ donating ability was found in the order $N^{3-} \gg NO < NS \approx NSe$ and the $\pi$ accepting ability in the order $NO > NS \approx NSe$. The weaker $\pi$ accepting ability of NS compared to NO results in a lower energy separation between the $1e(d_{yz,zx},\pi^*_{NE})$ and $2e(d_{yz,zx},\pi^*_{NE})^*$ sets of orbitals and between the $d_{xy}$ orbital and the $2e(d_{yz,zx},\pi^*_{NE})^*$ set of orbitals in the NS complexes in agreement with the optical absorption spectra and the values of $g_\perp$ obtained from the EPR spectra. The values of the isotropic and anisotropic hyperfine and superhyperfine coupling constants $A(^{53}Cr)$, $A(^{14}N)$, and $A(^{13}C)$ in the thionitrosyl complexes were slightly higher than in the analogous nitrosyl complexes. Spin populations generally show an NE ligand of increasing radical character through the series NO < NS < NSe with the change almost exclusively mediated by the chalcogen atom.

**Supporting Information Available:** Supporting Information (11 pp) includes tables of DFT calculations, Gaussian resolution of the optical absorption spectrum of $Cr(NO)(H_2O)_5^{2+}$, experimental and simulated EPR spectra of the complexes $Cr(NS)(nmf)_5^{2+}$, $Cr(NO)(nmf)_5^{2+}$, and $Cr(NO)(CN)_5^{3-}$ at 298 and 66 K. This material is available free of charge via the Internet at http://pubs.acs.org.

(51) Drago, R. S.; Meek, D. W.; Joesten, M. D.; Laroche, L. *Inorg. Chem.* **1963**, *2*, 124–127.